Published in final edited form as:
Clin Cancer Res. 2011 June 1; 17(11): 3638–3648. doi:10.1158/1078-0432.CCR-10-2456.

PDGF-D improves drug delivery and efficacy via vascular normalization, but promotes lymphatic metastasis by activating CXCR4 in breast cancer

Jieqiong Liu[1,2], **Shan Liao**[1], **Yuhui Huang**[1], **Rekha Samuel**[1], **Tony Shi**[3], **Kamila Naxerova**[1], **Peigen Huang**[1], **Walid Kamoun**[1], **Rakesh K. Jain**[1], **Dai Fukumura**[1], and **Lei Xu**[1]

[1] Edwin L. Steele Laboratory, Department of Radiation Oncology, Massachusetts General Hospital, Boston, Massachusetts 02114

[2] Department of Breast Surgery, the Second Xiangya Hospital of Central South University, Changsha, Hunan, China 410001

[3] College of Arts and Sciences, New York University, New York, NY 10012

Abstract

Purpose—Unlike Platelet-Derived Growth Factor-B (PDGF-B), the role of PDGF-D in tumor progression or treatment is largely unknown. To this end, we determined the role of PDGF-D in breast cancer progression, metastasis and response to chemotherapy.

Experimental Design—We first examined PDGF-D expression in human breast carcinomas by immunohistochemical (IHC) staining. To mimic high PDGF-D expressing tumors, we stably transfected the breast cancer cell lines MDA-MB-231 and 4T1 with *pdgf-d* cDNA, and implanted these tumor cells orthtopically into nude mice. We monitored tumor growth by caliper measurement and bioluminescence imaging. We also used short hairpin RNA interference (shRNAi) and imatinib to block PDGF-D/PDGFRβ signaling. Finally, we studied the effect of PDGF-D on doxorubicin delivery and efficacy.

Results—Human breast cancers express high levels of PDGF-D. Overexpression of PDGF-D promoted tumor growth and lymph node metastasis through increased proliferation, decreased apoptosis and induction of CXCR4 expression. Blockade of CXCR4 signaling abolished PDGF-D induced lymph node metastasis. Furthermore, overexpression of PDGF-D increased perivascular cell coverage and normalized tumor blood vessels. As a result, PDGF-D overexpression facilitated tissue penetration of doxorubicin and enhanced its treatment efficacy.

Conclusions—PDGF-D is highly expressed in human breast cancer and facilitates tumor growth and lymph node metastasis, making it a potential target in breast cancer. At the same time, PDGF-D increases drug delivery and hence improves the efficacy of chemotherapy through vessel normalization. Therefore, judicious use of PDGF-D/PDGFRβ blockers would be necessary to minimize the adverse effects on concomitantly administered cytotoxic therapies.

Introduction

Platelet-Derived Growth Factors (PDGFs) regulate many cellular processes including proliferation, apoptosis, transformation, migration, invasion, angiogenesis and metastasis. Four PDGF family members have been identified to date: the classical PDGF-A and -B are secreted as homodimers or heterodimers that bind to dimeric PDGF receptors composed of

Correspondence to: Lei Xu, MD, Ph.D. lei@steele.mgh.harvard.edu.

α- and/or β-chains. Unlike PDGF-A and -B, very little is known about PDGF-C and -D (1–3). PDGF-C can induce vascular normalization in GBM (4), and may be responsible for escape from anti-VEGF therapy (5). PDGF-D forms homodimers that are secreted in latent form and specifically bind to and activate PDGFR-β (2). PDGF-D has been found to be upregulated in prostate, lung, renal, ovarian, brain, and pancreatic cancers, and promotes their progression and metastasis (6–9). A recent study showed PDGF-D overexpression in breast tumor cells enhanced invasion *in vitro* (10). However, whether human breast tumors express PDGF-D and its role in breast cancer progression and treatment remains unexplored.

To reach cancer cells in a tumor, a blood-borne therapeutic agent must make its way across the blood vessel wall and subsequently diffuse through the tumor interstitium (11). Tumor vessels are structurally and functionally abnormal, and these vascular abnormalities lead to an abnormal tumor microenvironment characterized by interstitial hypertension, hypoxia, and acidosis, which in turn hinder delivery and efficacy of anti-tumor treatments (12). Blood vessels consist of vascular endothelial cells, perivascular cells (pericytes or vascular smooth muscle cells) and basement membrane. Recruitment of perivascular cells and their investment into newly formed blood vessels stabilizes these vessels, and their presence is necessary for vessel differentiation, maturation and function (13). PDGF-B/PDGFRβ signaling is critical for the recruitment of perivascular cells to vessel walls, and inhibition of PDGFRβ signaling has been shown to destabilize mature tumor vessels and increase metastasis (14–16). We have previously shown that overexpression of PDGF-D increases perivascular cell coverage in renal cell carcinoma (8), however, whether PDGF-D causes vessel maturation and improves drug delivery in breast carcinomas is not known.

In this study, we found that PDGF-D is strongly expressed in human breast cancers. Using an orthotopic breast cancer model in nude mice, overexpression of PDGF-D enhanced tumor progression and lymph node metastasis, whereas inhibition of PDGF-D signaling with imatinib and shRNAi inhibited tumor growth and metastasis. At the molecular level, PDGF-D led to activation of Akt and ERK1/2 MAPK. Furthermore, overexpression of PDGF-D increased CXCR4 expression in tumor tissues, which directly mediated PDGF-D-induced lymph node metastasis. Interestingly, overexpression of PDGF-D also led to higher perivascular cell coverage of tumor vessels and decreased vessel diameter. The ‘normalized’ tumor vessels improved the tumor tissue penetration of doxorubicin and enhanced its efficacy *in vivo*. These results provide novel insights into the contrasting roles and mechanisms of PDGF-D in progression and treatment of breast cancer and underscore the complexity of PDGFRβ blockade in cancer treatment.

Material and Methods

Cell Lines and Reagents

The mammary carcinoma cell lines MDA-MB-231, MDA-MB-435s, MDA-MB-468, BT474 and 4T1 cells, were obtained from the American Type Culture Collection (Manassas, VA). PDGF-D antibody and recombinant human PDGF-BB and PDGF-D protein were obtained from R&D Systems (Minneapolis, MN). Fluorescent doxorubicin hydrochloride and the CXCR4 antagonist AMD3100 were obtained from Sigma-Aldrich (St. Louis, MO). Doxorubicin was obtained from Novaplus (Irving, TX). Fluorescein lycopersion esculentum (Tomato) lectin (FITC-lectin) was obtained from Vector Laboratories (Burlingame, CA).

Plasmid Construct, Transfection and Infection

Full-length *pdgf-d* cDNA was cloned as described previously (8). This expression vector was stably transfected into MDA-MB-231 cells using Lipofectamine 2000 (Invitrogen,

Carisbad, CA) as instructed by the manufacturer. The transfected cells were selected with 0.5μg/ml puromycin.

Orthotopic Implantation of Tumor Cells

Viable MDA-MB-231 (5×10^6) and 4T1 (2×10^5) tumor cells suspended in 50 μl of Hank's Balanced Salt Solution (HBSS) were injected into the fourth left mammary fat pad of 8–12 week-old female nude mice. Tumor volume was calculated as: tumor volume = [length × $(\text{width})^2$]/2 (17). All animal procedures were performed following the guidelines of Public Health Service Policy on Humane Care of Laboratory Animals and approved by the Institutional Animal Care and Use Committee of the Massachusetts General Hospital.

Bioluminescence Imaging (BLI)

Cells were infected with lentivirus encoding both firefly luciferase (F-luc) and a DsRed reporter gene. DsRed positive cells were sorted with a FACSAria cell sorter (BD Biosciences, San Jose, CA). Mice implanted with F-luc tumor cells were anesthetized and injected with D-luciferin (Xenogen, 150 mg/kg, *i.p.*). Five minutes later, mice were placed in the IVIS Imaging System (Lumina II, Caliper Life Sciences, Hopkinton, MA). The image acquisition time ranged from 1 sec to 1 min. Post-processing and quantification was performed using Living Image software 3.0.

Western Blot Analysis

30 μg of protein per sample was separated on 10% SDS-polyacrylamide gels (18). Membranes were blotted with antibodies against: PDGFRβ (1:1000) and phospho-PDGFRβ (1:1000); p38 (1:1000) and phospho-p38 (1:1000); Akt (1:1000) and phospho-Akt (1:1000); ERK1/2 (1:1000) and phospho-ERK1/2 (1:1000). Antibodies were obtained from Cell Signaling (Beverly, MA).

RNA interference

PDGF-D shRNAi lentivirus was obtained from Santa Cruz Biotechnology (Santa Cruz, CA). MDA-MB-231 cells (1×10^5/well) were plated in flat-bottomed 48-well plates. Lentivial particles (MOI=5) and polybrene (8 μg/ml) were added into each well. The infected cells were selected with 0.5 μg/ml puromycin.

Immunohistochemistry

Tissue microarray slides (Biochain, Hayward, CA) was immunostained with anti-PDGF-D antibody (1:200, R&D Systems). The antibody stains specifically PDGF-D and does not cross-react with PDGF-A and PDGF-B. The anti-PDGF-D antibody also does not cross-react with recombinant human PDGF-C protein (R&D Systems) as determined by dot blot. Here we report PDGF-D staining as positive if a diffuse cytoplasmic staining was observed within cells. Internal positive controls in the tissues included endothelial cells, inflammatory cells and fibroblasts within the stroma serve as internal positive controls in the tissues. We scored cellular PDGF-D staining both qualitatively and quantitatively. For the former, intensity of staining was scored as follows: negative (if no staining was observed), weak, moderate and strong as compared with positive internal controls. For the quantitative scoring, we calculated percentage of PDGF-D positive cells among the total number of cells within the lesion.

Ki67 (Dako Ki67 kit, Capinteria, CA) staining was carried out on tissue sections of formalin-fixed, paraffin-embedded breast carcinoma xenografts. CD31 (1:250, BD Bioscience, Franklin Lake, NJ), F4/80 (1:200, Serotec, Raleigh, NC), NG2 (1:200, Sigma, St. Louis, MO), CXCR4 (1:100, Abcam, Cambridge, MA) and TUNEL (Millipore TUNEL

apoptosis detection kit, Billerica, MA) staining were carried out on frozen sections embedded in OCT compound (8 μm thick) (19).

Mammary Fat Pad Window and Multiphoton Laser Scanning Microscopy (MPLSM)

For non-invasive imaging of blood vessels in orthotopic breast cancers, tumor cells were implanted in mammary fat pad windows as described previously (20). Following implantation of the transparent access chamber, animals were allowed to recover for 48 hours before tumor implantation (5×10^6 cells/mice). Angiography was performed after intravenous injection of 50 μl of FITC-Dextran (10 mg/ml, 2,000 kDa, Sigma) as described previously. Vascular parameters were calculated using a semi-automated 3-D analysis system in ImageJ.

Transvascular Extravasation of Fluorescent Doxorubicin

50 μl fluorescent doxorubicin (15 mg/kg) was injected *i.v.* into the tail vein of tumor-bearing mice. Four hours later, 50 μl FITC-lectin (2 mg/kg) was injected *i.v.* to identify functional vessels. Five minutes later, tumors were resected and snap-frozen in liquid nitrogen. Three 20 μm thick sections, each 50 μm apart, were prepared. Images were taken using epifluorescence confocal microscopy. The extravasation pattern of fluorescent doxorubicin was analyzed using ImageJ (21).

Statistical Analysis

All data are presented as mean ± SD. The significance of differences between two groups was analyzed using the Student's *t* test (two-tailed) or Mann-Whitney *U* test (two-tailed).

Results

PDGF-D is highly expressed in human breast carcinomas

We first examined PDGF-D expression in human breast cancer tissue arrays. Tissue array slides contained 134 human breast carcinoma sections, 4 human breast fibroadenoma sections, 6 human mammary hyperplasia sections, and 6 normal human mammary gland sections (BioChain, Hayward, CA) (Supplemental Table 1). Using immunohistochemical staining, we observed that PDGF-D staining was positive in all the 134 human breast carcinoma cases examined. It was weakly or moderately expressed in the cytoplasm of epithelial and stromal cells of normal human mammary gland tissues and benign breast fibroadenomas (Fig. 1A). However, PDGF-D was homogenously and strongly expressed in carcinoma cells as well as in endothelial and stromal cells in invasive ductal carcinoma (Fig. 1B, Supplemental Table 2). We also found that expression of PDGF-D positively correlated with the expression of progesterone receptor (PR) ($P = 0.02$) and HER2 ($P = 0.0099$) (Supplemental Table 1, 2). It is noteworthy that no correlation between PDGF-D expression in the primary tumor and lymph node metastasis was found ($P=0.27$). Next, we examined whether established human breast cancer cell lines express PDGF-D and its receptor, PDGFRβ. In MDA-MB-435s, MDA-MB-231, MDA-MB-468, BT474 and 4T1 cells, both PDGF-D and PDGFRβ was detected by RT-PCR (Fig. 1C).

Overexpression of PDGF-D promotes growth and lymph node metastasis of orthotopic human breast cancer

To study the role of PDGF-D on tumor growth and metastasis, we cloned the full-length human *pdgf-d* cDNA (GenBank accession number: AF336376) and transfected it into MDA-MB-231 and 4T1 cells. Overexpression of PDGF-D was confirmed by quantitative RT-PCR (565-fold and 128 fold overexpression, respectively) and Western blot (Fig. 1D). Parental MDA-MB-231 and 4T1 cells expressed PDGFRβ protein, however activation of PDGFRβ

was barely detectable. In *pdgf-d* transfected cells (231-PDGFD and 4T1-PDGFD), PDGFRβ phosphorylation was clearly detected (Fig. 1D). PDGF-D overexpression did not change tumor cell proliferation (by MTT assay) or migration (by cell migration assay) *in vitro* (data not shown).

When implanted orthotopically, PDGF-D overexpressing MDA-MB-231 and 4T1 cells produced faster growing and larger tumors than the parental and mock-transfected cells (Fig. 2A, mock-data not shown). In parallel, we used bioluminescence imaging (BLI) to monitor tumor growth and metastasis in MDA-MB-231 tumors. We observed that orthotopically implanted 231-PDGFD tumors displayed significantly stronger firefly luciferase signals compared to parental 231 tumors (Fig. 2B). At the terminal point of the experiment, in mice bearing parental or PDGF-D transfected MDA-MB-231 tumors, we did not detect lung metastasis under dissecting microscope. Using bioluminescence imaging, we observed that all mice bearing 231-PDGFD tumors developed metastasis to inguinal and/or axiliary lymph nodes, whereas only 2 out of 8 mice bearing parental MDA-MB-231 tumors developed metastasis to the inguinal lymph node (Fig. 2C). Quantification of the luciferase signal confirmed that overexpression of PDGF-D significantly increased lymph node metastasis (Fig. 2C). In 4T1 tumors, overexpression of PDGF-D significantly increased lung metastasis (Fig. 2C).

Next, to study if inhibition of PDGF-D expression can inhibit tumor progression, we knocked down PDGF-D expression in MDA-MB-231 cells using lentiviral shRNAi. Decreased PDGF-D expression was confirmed by Western blot (data not shown). After orthotopic implantation, PDGF-D knocked-down tumor cells (231-PDGFD-si) produced slower growing and smaller tumors (Fig. 3A). Bioluminescence imaging study showed that the lymph node metastases also decreased significantly (2.2 ± 1.68 million photon/sec in parental MDA-MB-231 mice vs. 0.14 ± 0.03 million photon/sec in 231-PDGFD-si mice). The inhibition of PDGF-D expression in orthotopic breast cancer tissues was confirmed by IHC (data not shown).

Finally, we blocked PDGFRβ signaling using imatinib, an inhibitor against PDGFRβ tyrosine kinase, c-kit and bcr-abl. Treatment began 10 days following tumor implantation. Daily oral gavage of imatinib for 30 days did not affect body weight (data not shown). In parental MDA-MB-231 tumors, which does not express phosphorylated PDGFRβ, imatinib treatment was not effective in inhibiting tumor growth. In PDGF-D overexpressing MDA-MB-231 tumors, which express phosphorylated PDGFRβ, imatinib significantly inhibited tumor growth (Fig. 3B–C).

PDGF-D increases tumor cell proliferation and inhibits tumor cell apoptosis in breast cancer via activation of MAPK and Akt signaling pathways

We analyzed tumor cell proliferation and apoptosis by Ki67 and TUNEL staining of tumor tissues. We found that 231-PDGFD tumors had a higher cell proliferation rate (34.5 ± 3.3) compared to parental tumors (24.5 ± 4.1) ($P < 0.05$, data shown as number of $Ki67^+$ cells per 0.041 mm^2). In addition, 231-PDGFD tumors showed significantly lower rates of cell apoptosis (9.9 ± 3.5) compared to parental tumors (53.1 ± 20.4, $P < 0.05$, data are shown as number of $TUNEL^+$ cells per 0.329 mm^2).

It has been shown that ERK1/2 and p38 MAPK induce the mitogenic signal, and Akt mediates the anti-apoptotic signal generated by PDGF-B/PDGFRβ (22–23). Given that PDGF-D shares the PDGFRβ receptor with PDGF-B, we therefore sought to determine whether MAPK and Akt are activated in PDGF-D overexpressing tumors. We found that phosphorylated ERK1/2, p38, and Akt levels increased significantly in 231-PDGFD tumors, while no change in the levels of total ERK, p38 or Akt was detected (Fig. 3D).

PDGF-D enhances lymph node metastasis via SDF-1α/CXCR4 axis

Increased lymphangiogenesis has been shown to enhance the rate of tumor cell metastasis to lymph nodes (24). PDGF-BB has been shown to induce tumor lymphangiogenesis, leading to enhanced metastasis in lymph nodes (25). However, we could not detect differential expression of VEGF-C or LYVE-1 in parental MDA-MB-231, 231-PDGFD and 231-PDsi tumors. These data suggest that increase in lymph node metastasis induced by PDGF-D is mediated by a mechanism independent of lymphangiogenesis. The SDF-1α/CXCR4 chemokine axis has been shown to play a critical role in breast cancer metastasis (26). Using qRT-PCR and IHC, we examined SDF1α and CXCR4 expression in PDGF-D transfected cells and tumors. Overexpression of PDGF-D did not change SDF-1α or CXCR4 expression *in vitro* (data not shown). However, 231-PDGFD tumors had significantly higher CXCR4 expression at both mRNA (a 6-fold increase) and protein levels (Fig. 4A–B).

To examine whether the SDF-1α/CXCR4 pathway directly mediates PDGF-D-induced metastasis, we treated the mice bearing 231 or 231-PDGFD tumors with a CXCR4 antagonist, AMD3100. AMD3100 treatment did not change the primary tumor growth of either parental or 231-PDGFD tumors (Fig. 4C), but it significantly decreased lymph node metastasis in the 231-PDGFD group (Fig. 4D).

PDGF-D normalizes tumor vasculature

We analyzed tumor vessel density and perivascular cell coverage by CD31 and NG2 double fluorescent staining. We observed no significant difference in blood vessel density between parental (24.2 ± 2.5) and 231-PDGFD tumors (29.3 ± 7.3, data shown as number of $CD31^+$ structures per 1.355 mm^2). However, we found the fraction of vessels covered by NG2-positive perivascular cells increased from 32.2% in 231-parental tumors to 78.7% in 231-PDGFD tumors (Fig. 5A). Using multiphoton laser scanning microcopy, we studied the vascular morphology of tumors grown in mammary fat pad chambers. In parental tumors, we observed tortuous and abnormally dilated vessels as typically seen in solid tumors. In 231-PDGFD tumors, we observed a reduction in vessel diameter and a shift towards a more anatomically normal phenotype (Fig. 5B).

PDGF-D improves the tumor tissue penetration of doxorubicin and its efficacy

Since PDGF-D overexpression morphologically normalized the tumor vasculature, we determined if PDGF-D can increase tissue penetration of doxorubicin, a fluorescent chemotheraputic drug (Fig. 5C). The average intensity of extravasated fluorescent doxorubicin was quantified as a function of distance from the blood vessel wall. Quantitative analysis showed that fluorescent doxorubicin penetrated significantly deeper in 231-PDGFD tumors (24.1 ± 9.2 μm) than in parental 231 tumors (7.1 ± 2.3 μm) (Fig. 5C).

Finally, we studied whether PDGF-D enhances the efficacy of doxorubicin. Doxorubicin treatment started 14 days after orthotopic implantation, and continued weekly for 3 weeks. Inguinal and axillary lymph nodes were collected at the end of the experiment for bioluminescence imaging. Doxorubicin treatment was significantly more effective in inhibiting the growth and lymph node metastasis of 231-PDGFD tumors than in parental groups (Fig. 6A–C).

Discussion

The PDGF-B/Rβ signaling pathway has been characterized in invasive breast cancer. PDGFRα and β are commonly overexpressed both in tumor and stromal cells (27), and PDGF receptor β has been shown to be upregulated in breast cancer endothelial cells (28). Autocrine PDGFR signaling has been shown to promote breast cancer metastasis (29).

PDGF-D is the most recent addition to the PDGF family (10). Whether PDGF-D is expressed in human breast cancer tissues and whether it affects tumor growth and metastasis *in vivo* are not known. In this study, we observed for the first time that PDGF-D is highly expressed in human breast cancers. We found that overexpression of PDGF-D activates the PDGFRβ signaling and enhances tumor growth and metastasis. We then, blocked PDGF-D signaling using both genetic (shRNA) and pharmacological (imatinib) approaches. We observed that PDGF-D knockdown decreased tumor growth, but inhibition of PDGFRβ by imatinib has only minimal effect on parental MDA-MB-231 tumor growth. The efficacy of the pharmacological approach may be reduced due to the abnormal tumor microenvironment resulting in decreased drug delivery. However, it is also possible that PDGF-D exerts its pro-tumor effects via other signaling pathways. Indeed, recent studies reported PDGF-D crosstalk with PI3K/Akt, Notch and NF-κB signaling pathways and increased tumor angiogenesis and invasion (7, 10, 22). In summary, we conclude that although PDGF-D pathway alone does not provide a sufficient autocrine signal to accelerate MDA-MB-231 cell growth *in vitro*, it potentiates tumor growth and metastasis *in vivo* via: (i) stimulation of cancer cell proliferation through ERK1/2 and p38 MAPK activation, (ii) protection of cancer cells from apoptosis via Akt activation, and (iii) stimulation of tumor cell metastasis via activation of SDF-1α/CXCR4 pathway.

Others and we have previously shown that overexpression of PDGF-D increased tumor metastasis in renal cell carcinoma (8) and PDGF-D contributes to epithelial-mesenchymal transition (EMT) phenotype in prostate cancer cells (30). Here, we show a novel mechanism by which PDGF-D enhances metastasis. We found that overexpression of PDGF-D increase nodal metastasis of orthotopic MDA-MB-231 breast carcinomas via CXCR4 signaling. Blocking CXCR4 with AMD3100, a specific inhibitor of CXCR4, abolished PDGF-D-induced metastasis, suggesting that CXCR4 signaling directly mediates PDGF-D induced metastasis. A growing body of literature has indicated that SDF-1α/CXCR4 pathway plays a critical role in cancer cell metastasis (31). CXCR4 expression level in human breast cancers is positively correlated with lymph node metastasis and inversely correlated with patient prognosis (32, 33). In our study, we observed PDGF-D increased CXCR4 in tumor tissues but not in tumor cells in culture, suggesting that PDGF-D in tumor microenvironment either indirectly upregulates CXCR4 expression or increases recruitment of CXCR4 expressing stromal cells. Further study is needed to dissect the mechanism of PDGF-D induced CXCR4 expression and pinpoint the cell type in which CXCR4 is upregulated.

Another important finding of this study is that overexpression of PDGF-D improves the delivery and efficacy of cytotoxic therapies via normalization of tumor vasculature. In breast cancer, VEGF and PDGF families have been identified as angiogenic factors (34, 35). PDGF-D has been shown to upregulate VEGF and to stimulate angiogenesis (36). In our study, overexpression of PDGF-D did not change VEGF expression in tumor cells or in host tissues (data not shown). As a result, we did not observe differences in tumor angiogenesis between parental and PDGF-D overexpressing tumors. However, we found that PDGF-D overexpression normalized tumor blood vessel morphology and increased perivascular cell coverage. This vessel maturation can attenuate vascular hyperpermeability, lower tumor interstitial fluid pressure (IFP), and restore pressure gradients across vessel walls as well as into tissues (20). As a result, tissue penetration of chemotherapeutic agents is improved (20). In some cases, blocking PDGFR signaling by imatinib has been shown to lower IFP (37), presumably via different mechanisms, such as fibroblast contraction. In this study, we showed that PDGF-D could normalize vessel function and increase the penetration of chemotherapeutic agents and ultimately improve the efficacy of anti-tumor therapy in an orthotopic breast cancer model, suggesting a new strategy for enhancing the effects of chemotherapy.

In summary, PDGF-D is highly expressed in human breast carcinoma tissues. On one hand, overexpression of PDGF-D leads to increased tumor growth and metastasis; on the other hand, overexpression of PDGF-D normalizes tumor blood vessels and improves delivery and efficacy of chemotherapeutic drugs. Our preclinical study suggests that PDGFR-β blockers should be used cautiously, especially in combination with chemotherapy in the clinic. For example, in patients with high levels of PDGF-D in tumors, imatinib treatment should be avoided at the time of cytotoxic therapy. Future studies are thus necessary to explore the risks and benefits of PDGFR-β blockade for anticancer treatment.

Supplementary Material

Refer to Web version on PubMed Central for supplementary material.

Acknowledgments

We thank Dr. Gang Cheng, Dannie Wang, Julia Kahn, and Carolyn Smith for their superb technical support.

Grant support: This study was supported in part by Clafflin Distinguished Scholar Award, Harvard Medical School (LX), US National Cancer Institute grants P01-CA80124 (RKJ and DF), R01-CA85140 (RKJ), R01-CA96915 (DF), R01-CA115767 (RKJ), R01-CA126642 (RKJ) and US Department of Defense Breast Cancer Research Innovator Award - W81XWH-10-1-0016 (RKJ).

References

1. Li X, Ponten A, Aase K, et al. PDGF-C is a new protease-activated ligand for the PDGF alpha-receptor. Nat Cell Biol. 2000; 2:302–9. [PubMed: 10806482]
2. LaRochelle WJ, Jeffers M, McDonald WF, et al. PDGF-D, a new protease-activated growth factor. Nat Cell Biol. 2001; 3:517–21. [PubMed: 11331882]
3. Bergsten E, Uutela M, Li X, et al. PDGF-D is a specific, protease-activated ligand for the PDGF beta-receptor. Nat Cell Biol. 2001; 3:512–6. [PubMed: 11331881]
4. di Tomaso E, London N, Fuja D, et al. PDGF-C induces maturation of blood vessels in a model of glioblastoma and attenuates the response to anti-VEGF treatment. PLoS One. 2009; 4:e5123. [PubMed: 19352490]
5. Crawford Y, Kasman I, Yu L, et al. PDGF-C mediates the angiogenic and tumorigenic properties of fibroblasts associated with tumors refractory to anti-VEGF treatment. Cancer Cell. 2009; 15:21–34. [PubMed: 19111878]
6. Ustach CV, Taube ME, Hurst NJ Jr, et al. A potential oncogenic activity of platelet-derived growth factor D in prostate cancer progression. Cancer Res. 2004; 64:1722–9. [PubMed: 14996732]
7. Wang Z, Kong D, Banerjee S, et al. Down-regulation of platelet-derived growth factor-D inhibits cell growth and angiogenesis through inactivation of Notch-1 and nuclear factor-kappaB signaling. Cancer Res. 2007; 67:11377–85. [PubMed: 18056465]
8. Xu L, Tong R, Cochran DM, Jain RK. Blocking platelet-derived growth factor-D/platelet-derived growth factor receptor beta signaling inhibits human renal cell carcinoma progression in an orthotopic mouse model. Cancer Res. 2005; 65:5711–9. [PubMed: 15994946]
9. LaRochelle WJ, Jeffers M, Corvalan JR, et al. Platelet-derived growth factor D: tumorigenicity in mice and dysregulated expression in human cancer. Cancer Res. 2002; 62:2468–73. [PubMed: 11980634]
10. Ahmad A, Wang Z, Kong D, et al. Platelet-derived growth factor-D contributes to aggressiveness of breast cancer cells by up-regulating Notch and NF-kappaB signaling pathways. Breast Cancer Res Treat. 2011; 126:15–25. [PubMed: 20379844]
11. Jain RK, Stylianopoulos T. Delivering nanomedicine to solid tumors. Nat Rev Clin Oncol. 2010; 7:653–64. [PubMed: 20838415]
12. Jain RK. Normalization of tumor vasculature: an emerging concept in antiangiogenic therapy. Science. 2005; 307:58–62. [PubMed: 15637262]

13. Hirschi KK, D'Amore PA. Pericytes in the microvasculature. Cardiovasc Res. 1996; 32:687–98. [PubMed: 8915187]
14. Jain RK. Molecular regulation of vessel maturation. Nat Med. 2003; 9:685–93. [PubMed: 12778167]
15. Jain RK, Booth MF. What brings pericytes to tumor vessels? J Clin Invest. 2003; 112:1134–6. [PubMed: 14561696]
16. Gerhardt H, Semb H. Pericytes: gatekeepers in tumor cell metastasis? J Mol Med. 2008; 86:135–42. [PubMed: 17891366]
17. Xu L, Yoneda J, Herrera C, Wood J, Killion JJ, Fidler IJ. Inhibition of malignant ascites and growth of human ovarian carcinoma by oral administration of a potent inhibitor of the vascular endothelial growth factor receptor tyrosine kinases. Int J Oncol. 2000; 16:445–54. [PubMed: 10675474]
18. Xu L, Pathak PS, Fukumura D. Hypoxia-induced activation of p38 mitogen-activated protein kinase and phosphatidylinositol 3′-kinase signaling pathways contributes to expression of interleukin 8 in human ovarian carcinoma cells. Clin Cancer Res. 2004; 10:701–7. [PubMed: 14760093]
19. Xu L, Cochran DM, Tong RT, Winkler F, Kashiwagi S, Jain RK, Fukumura D. Placenta Growth Factor overexpression inhibits tumor growth, angiogenesis, and metastasis by depleting Vascular Endothelial Growth Factor homodimers in orthotopic mouse models. Cancer Res. 2006; 66:3971–77. [PubMed: 16618713]
20. Jain, RK.; Brown, E.; Munn, L.; Fukumura, D. Intravital Microscopy of Normal and Diseased Tissues in the Mouse. In: Robert, D.; Goldman, JRS.; Spector, David L., editors. Live Cell Imaging: A Laboratory Manual. 2. NY: Cold Spring Harbor Laboratory; 2010. p. 475-522.
21. Tong RT, Boucher Y, Kozin SV, Winkler F, Hicklin DJ, Jain RK. Vascular normalization by vascular endothelial growth factor receptor 2 blockade induces a pressure gradient across the vasculature and improves drug penetration in tumors. Cancer Res. 2004; 64:3731–6. [PubMed: 15172975]
22. Kong D, Banerjee S, Huang W, et al. Mammalian target of rapamycin repression by 3,3′-diindolylmethane inhibits invasion and angiogenesis in platelet-derived growth factor-D-overexpressing PC3 cells. Can Res. 2008; 68:1927–34.
23. Dudek H, Datta SR, Franke TF, et al. Regulation of neuronal survival by the serine-threonine protein kinase Akt. Science. 1997; 275:661–5. [PubMed: 9005851]
24. Hoshida T, Isaka N, Hagendoorn J, et al. Imaging steps of lymphatic metastasis reveals that vascular endothelial growth factor-C increases metastasis by increasing delivery of cancer cells to lymph nodes: therapeutic implications. Cancer Res. 2006; 66:8065–75. [PubMed: 16912183]
25. Cao R, Bjorndahl MA, Religa P, et al. PDGF-BB induces intratumoral lymphangiogenesis and promotes lymphatic metastasis. Cancer Cell. 2004; 6:333–45. [PubMed: 15488757]
26. Luker KE, Luker GD. Functions of CXCL12 and CXCR4 in breast cancer. Cancer Lett. 2006; 238:30–41. [PubMed: 16046252]
27. Coltrera MD, Wang J, Porter PL, Gown AM. Expression of platelet-derived growth factor B-chain and the platelet-derived growth factor receptor beta subunit in human breast tissue and breast carcinoma. Cancer Res. 1995; 55:2703–8. [PubMed: 7780988]
28. Vrekoussis T, Stathopoulos EN, Kafousi M, Navrozoglou I, Zoras O. Expression of endothelial PDGF receptors alpha and beta in breast cancer: up-regulation of endothelial PDGF receptor beta. Oncol Rep. 2007; 17:1115–9. [PubMed: 17390053]
29. Jechlinger M, Sommer A, Moriggl R, et al. Autocrine PDGFR signaling promotes mammary cancer metastasis. J Clin Invest. 2006; 116:1561–70. [PubMed: 16741576]
30. Rahman KM, Banerjee S, Ali S, et al. 3,3′-Diindolylmethane enhances taxotere-induced apoptosis in hormone-refractory prostate cancer cells through survivin down-regulation. Cancer Res. 2009; 69:4468–75. [PubMed: 19435906]
31. Muller A, Homey B, Soto H, et al. Involvement of chemokine receptors in breast cancer metastasis. Nature. 2001; 410:50–6. [PubMed: 11242036]

32. Yasuoka H, Tsujimoto M, Yoshidome K, et al. Cytoplasmic CXCR4 expression in breast cancer: induction by nitric oxide and correlation with lymph node metastasis and poor prognosis. BMC Cancer. 2008; 8:340. [PubMed: 19025611]

33. Kang H, Watkins G, Douglas-Jones A, Mansel RE, Jiang WG. The elevated level of CXCR4 is correlated with nodal metastasis of human breast cancer. Breast. 2005; 14:360–7. [PubMed: 16216737]

34. Rice A, Quinn CM. Angiogenesis, thrombospondin, and ductal carcinoma in situ of the breast. J Clin Pathol. 2002; 55:569–74. [PubMed: 12147647]

35. Brown LF, Guidi AJ, Schnitt SJ, et al. Vascular stroma formation in carcinoma in situ, invasive carcinoma, and metastatic carcinoma of the breast. Clin Cancer Res. 1999; 5:1041–56. [PubMed: 10353737]

36. Li H, Fredriksson L, Li X, Eriksson U. PDGF-D is a potent transforming and angiogenic growth factor. Oncogene. 2003; 22:1501–10. [PubMed: 12629513]

37. Pietras K, Rubin K, Sjoblom T, et al. Inhibition of PDGF receptor signaling in tumor stroma enhances antitumor effect of chemotherapy. Cancer Res. 2002; 62:5476–84. [PubMed: 12359756]

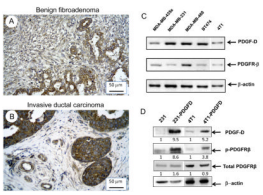

Figure 1.

Immunohistochemical staining of PDGFD (1:250) in (A) breast fibroadenoma tissue, (B) invasive ductal breast carcinoma tissue (20X). (C) RT-PCR analysis of PDGF-D and PDGFRβ in breast cancer cell lines: MDA-MB-435s, MDA-MB-231, MDA-MB-468, BT474 and 4T1. (D) Western blot analysis of PDGFD, phosphorylated and total PDGFRβ in parental and PDGFD transfected MDA-MB-231 and 4T1 cells. Densitometry data was calculated by normalizing the PDGF-D, total and phosphorylated PDGFRβ intensity to that of β-actin using NIH Image.

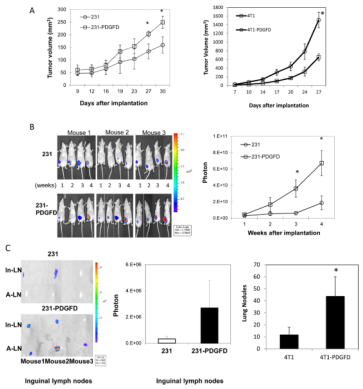

Figure 2.

(A) Parental and PDGF-D transfected MDA-MB-231 and 4T1 cells were injected into the fourth left mammary fat pad of nude mice, tumor size was measured every 3 days ($n = 8$, $P < 0.005$). (B) Representative bioluminescence images (BLI) of mice bearing parental (231) and PDGF-D transfected (231-PDGFD) MDA-MB-231 tumors. BLI study started 7 days after tumor implantation and was performed weekly to monitor the development of tumors. Signal intensity is measured as photon flux (photons/second) and coded to a color scale. (C) Thirty days after tumor implantation, mice bearing parental and PDGF-D transfected MDA-MB-231 tumors were sacrificed. Inguinal (In-LN) and axillary (A-LN) lymph nodes were collected for BLI study ($n = 8$). BLI images were quantified using Living Image software 3.0. $P < 0.005$. Lungs were collected from mice bearing parental and PDGF-D transfected 4T1 tumors, metastatic nodules were counted under dissecting microscope.

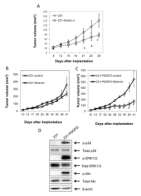

Figure 3.

(A) Parental (231), mock (data not shown) or PDGFD-shRNAi infected MDA-MB-231 cells (231-PDGFD-si) were injected into the fourth left mammary fat pad of nude mice. All mice were sacrificed on day 29. Tumor size was measured by caliper every 3 days ($n = 8$, $P < 0.005$). Ten days after implantation of (B) parental 231 or (C) 231-PDGFD cells, mice were randomized to receive one of the following treatments by oral gavage daily: water (control), or imatinib (100 mg/kg). Mice were sacrificed on day 41 after implantation. Tumor size was measured every 3 days by caliper ($n = 8$, $P < 0.005$). (D) Western blot analysis of phosphorylated and total p38, Akt, ERK1/2.

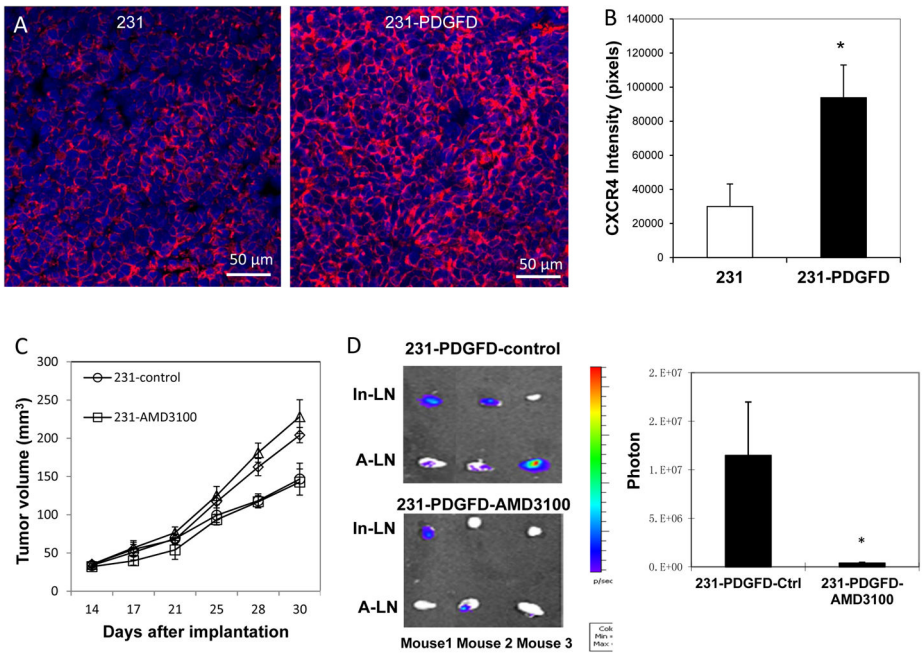

Figure 4.

(A) Immunofluorescent staining of CXCR4 in parental MDA-MB-231 and 231-PDGFD tumor tissues (20x). (B) Quantification of CXCR4 staining intensity by ImageJ. $P < 0.01$. (C) Fourteen days after orthotopic implantation, mice were randomized to be implanted subcutaneously with a 14-day continuous release osmotic pump (Alzet®, Cupertino, CA) containing saline (control), or AMD3100 (7 mg/kg/day) (n = 8). Tumor size was measured every three days by caliper. Mice were sacrificed on day 30, and (D) inguinal (In-LN) and axillary (A-LN) lymph nodes were collected for BLI study. BLI images were quantified using Living Image software 3.0. $P < 0.005$.

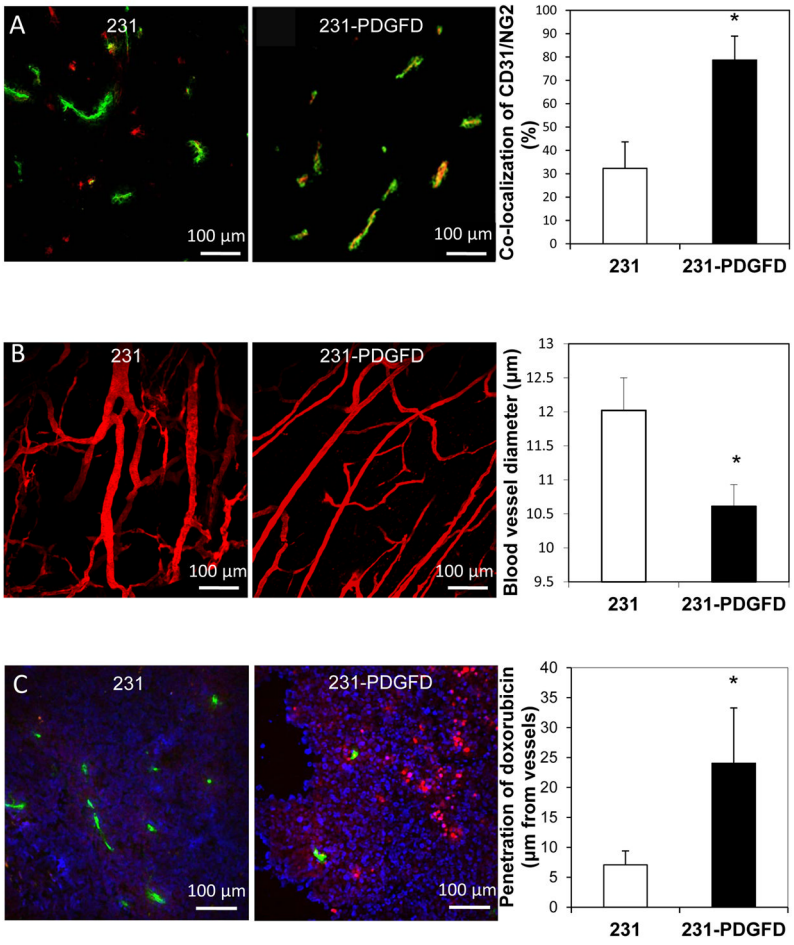

Figure 5.

(A) Immunofluorescence double staining for endothelial cells (CD31, green) and perivascular cells (NG2, red) in frozen sections of parental (231) and 231-PDGFD tumors. The percentage of CD31 and NG2 co-localization was quantified using ImageJ. $P < 0.05$. (B) Angiographic images of blood vessels in parental tumor (231), and 231-PDGFD tumors implanted in the mammary fat pad chamber were captured using mutiphoton laser scanning microscopy (MPLSM). Blood vessel diameter was quantified using a semi-automated 3-D analysis system. $P < 0.05$. (C) Extravasation of fluorescent doxorubicin (red) from perfused vessels (FITC-lectin, green) was examined in parental (231) and 231-PDGFD tumors. An automated routine in ImageJ was used to quantify the average intensity of extravasted fluorescent doxorubicin as a function of distance from the blood vessel wall (n = 12 sections; 3 sections per tumor; Image width: 512 μm, $P < 0.05$).

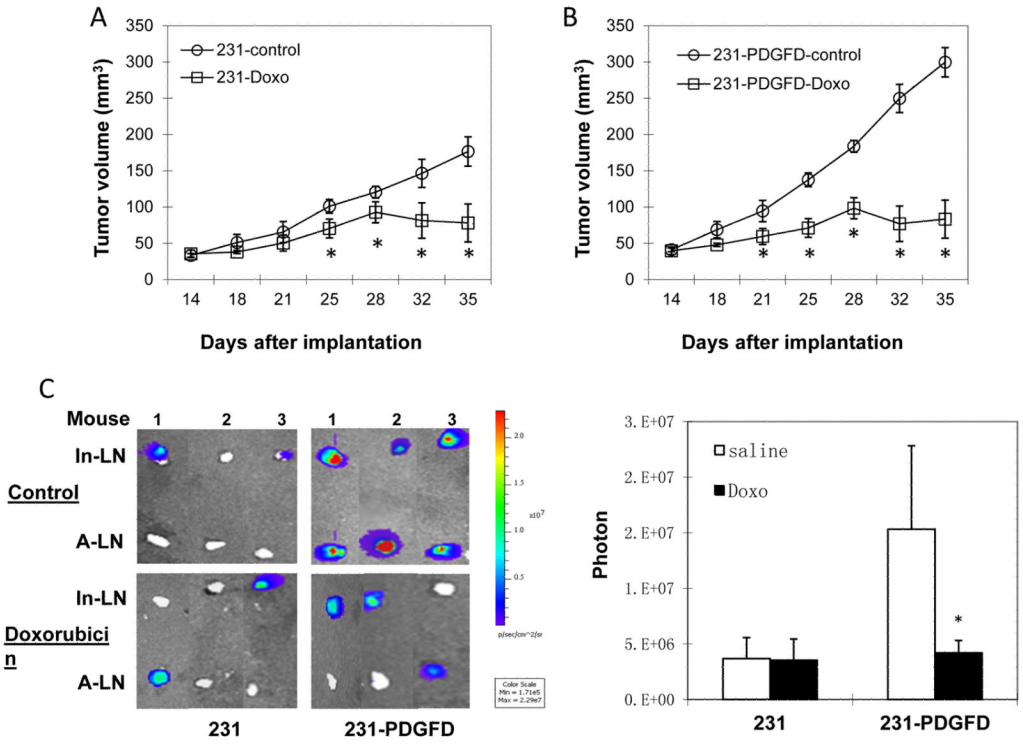

Figure 6.

(A) Parental (231) and (B) 231-PDGFD tumor cells were implanted orthotopically. Fourteen days after orthotopic implantation, mice were randomized to receive weekly *i.p.* injection of saline (control) or doxorubicin (Doxo, 5 mg/kg, n=8, $P < 0.05$). Tumor was measured every three days by caliper. Mice were sacrificed on day 35. (C) Representative BLI images of inguinal and axillary lymph nodes (n = 8). BLI images were quantified using Living Image software 3.0. $P < 0.005$.